From the Study of Table Trajectories during Collaborative Carriages toward Pro-active Human-Robot Table Handling Tasks

Isabelle Maroger, Olivier Stasse, Bruno Watier

From the Study of Table Trajectories during Collaborative Carriages toward Pro-active Human-Robot Table Handling Tasks

Isabelle Maroger[1] and Olivier Stasse[1] and Bruno Watier[1]

***Abstract*— The study of human-human interactions is essential for a better understanding of human behaviour during collaborative tasks. This knowledge is not only interesting in life science but can also be useful in robotic science. Indeed, to efficiently assist a human partner during a human-robot collaboration, the robot needs to be as reactive as a human would be. This can only be achieved by embedding a model of human behaviour into the robot control scheme. In this paper, a human-humanoid robot collaboration to carry a table is tackled. First, the experimental Center of Mass (CoM) trajectories of a table carried by 20 pairs of subjects to various goal positions are studied and modeled using an optimal control problem. Then, based on this model, a prediction process which accurately predicts the table trajectories is designed. Finally, this prediction process is coupled with the robot Walking Pattern Generator (WPG). Using a torque whole-body controller, this framework is tested in simulation on Gazebo on a TALOS humanoid robot model. In this simulation, the robot actively assists a simulated human partner in lifting and carrying a table to an unknown goal position.**

I. Introduction

In the context of the growing number of robots in the industrial world or even in people's daily lives, Human-Robot Interaction (HRI) is a booming field of study [1], [2]. However, achieving a successful and useful HRI is far from easy, especially when dealing with humanoid robots. Indeed, these robots are complex to control and might be harmful to a human partner due to their heavy weight and wide range of motions. Moreover, due to the redundancy of the musculoskeletal system of humans, there is a large variability of motions for a given task between individuals and the robot should be able to adapt to every human partner. Thus, making a humanoid robot interact with a human partner requires a safe and robust controller along with an effective and adaptive planner. This work, carried out as part of the ANR-CoBot project, focuses on a specific physical Human-Robot Interaction (pHRI): a table handling task in collaboration with a humanoid TALOS robot built by *PAL Robotics* and a human partner. The goal is to build and embed a real-time prediction model of the table trajectories during carriage tasks in the robot Walking Pattern Generator (WPG). In doing so, the footsteps are expected to be more reactive and, thus, the humanoid robot may be more useful to assist a human in carrying a table.

A. Related works

1) Study of human collaboration to improve HRI: Even if there is a significant variability inherent in human movements [3], humans have the ability to quickly adapt their behaviour when collaborating with others. They can even predict their partners' intentions using visual, verbal and haptic signals. To move towards efficient HRI, the robots have to be as reactive as human beings. This is why numerous works study human collaboration in order to improve HRI. For example, [4] studied a beam transportation task. They measured the postures of the subjects and the forces and torques applied on the beam while being carried by two subjects. From those measurements, they proposed a control scheme for physical interactions for a HRP-2 robot. [5] also performed human-human experiments to carry a beam. Using a multiclass classification problem, they developed an algorithm which detected human's intentions while walking with a beam and embedded it in a COMAN robot controller to make it more pro-active during beam transportation with a human partner. Furthermore, the goal of some studies in the HRI field is to enable robots to actively assist a human during collaborative tasks. One solution, proposed by [6], was to reconstruct a pre-recorded human motion and replicate it on the robot. This work resulted in a simulation of a collaborative pick-and-place experiment where a HRP-4 robot assisted its partner in a human-like manner. This demonstrated the ability to mimic human motions on a humanoid robot. However, this method demanded an initial recording of a human motion, which prevented real-time applications.

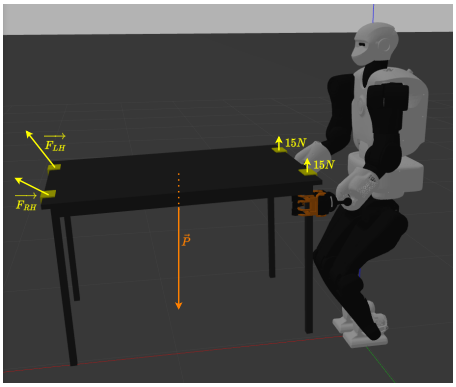

Fig. 1. Simulation on Gazebo where a TALOS humanoid robot holds a 20.7 kg table. $\vec{P}$ is the weight of the table. $\overrightarrow{F}_{RH}$ and $\overrightarrow{F_{LH}}$ are the forces applied on the left yellow spots to simulate the forces applied on the table by the hands of the human partner.

2) pHRI: Two main strategies exist to deal with pHRI [1].

The first classic approach is to use impedance control [7], [8], [9]. However, this approach usually considers the human partner as a perturbation. By doing so, the robot is the leader

*This work was supported by the grant ANR-COBOT [18CE10-0003].
[1]LAAS-CNRS, Université de Toulouse, CNRS, UPS, Toulouse, France
{imaroger,ostasse,bwatier}@laas.fr

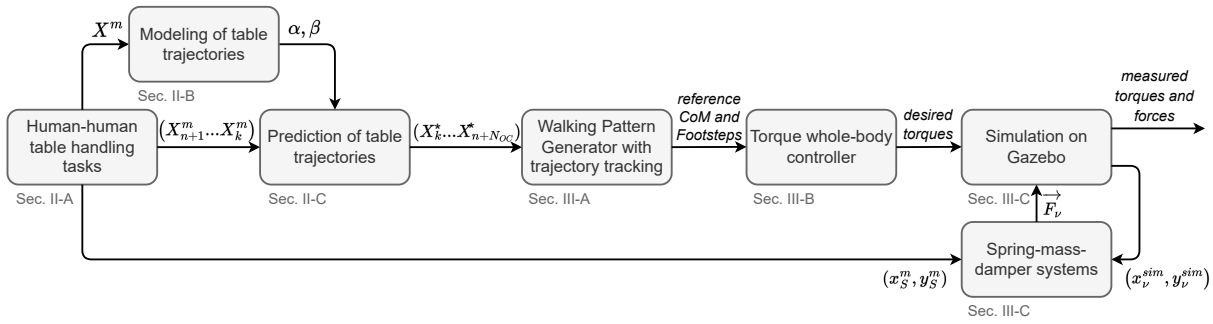

Fig. 2. Description of the whole framework presented in this paper. The notations introduced in this chart are defined throughout the paper.

of the motion instead of assisting the human to do the motion. Impedance control can also be used to copy [10] or learn [11] human control. For example, in [11], the authors made a robot "learn" a task during a pHRI. In this work, a HRP-2 robot collaborated with a human partner to lift a beam only through haptic feedback. Those demonstrations were recorded and used by a learning model based on a Gaussian mixture model in order to make the robot as reactive as a human being when performing this task.

The other method focused on the prediction of human intentions to adapt the robot's behaviour to its partner's motions [12]. For example, [13] performed a transportation task where a HRP-2 robot guessed its partner's intentions using motion primitives (stop, walk, side, turn). In this work, the prediction of the human's intentions was based on the velocity of the human partner. However, other criteria, such as the velocity transmission of a robot arms [14], the measurements of the contact forces with a robotic skin [15] or the human past trajectory [16], could be used to predict the human's motions as part of HRI. In this paper, this approach was chosen as it was successfully implemented in numerous works to perform pHRI with a pro-active robot.

B. Contributions

A human-humanoid robot collaborative table handling task is tackled in this paper. To achieve this goal, we implemented the framework presented in Fig.2. The main contributions of this paper are threefold. First, it provides a short analysis of the experimental trajectories performed by a table handled by two subjects. Previous work [17] already showed that the trajectories performed by the subjects are too diverse to be simulated with the same method used to simulate single walking humans [18]. Thus, the present work focuses on the analysis of the table trajectories in order to investigate the variability of those trajectories and the possibility to model the table behaviour instead of the subjects' behaviour. Then, in this article, we demonstrate that the same method can be applied to model and predict the Center of Mass (CoM) table trajectories during carriage tasks as well as to model and real-time predict the CoM trajectories of single walking human [18], [19], [16]. Once the prediction model is built, it is embedded in the WPG of the TALOS humanoid robot as in [16]. Finally, this work proposes a simulation of a table carried by a robot on one side and a simulated human on the other side, as Fig.1 shows. This simulation is aimed to be as realistic as possible. Thus, in simulation, a TALOS humanoid robot is able to actively carry a 20.7 kg table without losing its balance or performing sharp motions which could endanger its simulated partner.

II. Modeling and Prediction of the Table Trajectories

A. Experiments

1) Participants: Forty healthy subjects (15 females and 25 males) volunteered to perform table handling tasks. They ranged from 19 to 46 years old (average 26.7 ± 5.9), their heights from 1.6 m to 1.99 m (average 1.76 ± 0.09) and their masses from 54 kg to 108 kg (average 71.7 ± 14.6). They were randomly put into 20 pairs to take part in the experiments. Before their participation, each subject was informed of the experimental protocol and gave his written consent. Those experiments were conducted in accordance with the declaration of Helsinki and were approved by the University of Toulouse ethical committee.

2) Experimental protocol: First of all, before taking part in the experiments, the pair's members were randomly named *Subject 1* and *Subject 2*. This appointment determined on which side of the table the subjects had to stand at the beginning of each trial. However, no guidelines were given on whether the subjects had to face the table or stand their back to it. Then, the subjects were asked to carry a 20.7 kg table back and forth from one starting position to 9 different goal positions. Those goal positions are represented in Fig.3. They were chosen to be representative of common carriages over distances from 2.7 m to 5.4 m. During the experiments presented in this paper, both subjects were informed of the next goal position before each trial. The goal positions were marked with 4 pieces of adhesive tape on the floor, one for each table leg. There were no guidelines about where the subjects should stand at the end of the handling task. In this study, the path the pair took to go to the goal position is named *forward path* and the path it took to come back to the starting position is named *return path*.

3) Data collection and processing: Four reflective passive markers were placed on the subjects' pelvis, on the postero-superior iliac spines and 2 on the antero-superior iliac spines. Three markers were placed on 3 of the 4 corners of the table to reconstruct a local frame. The 3D positions of those markers were recorded using a motion capture system (15

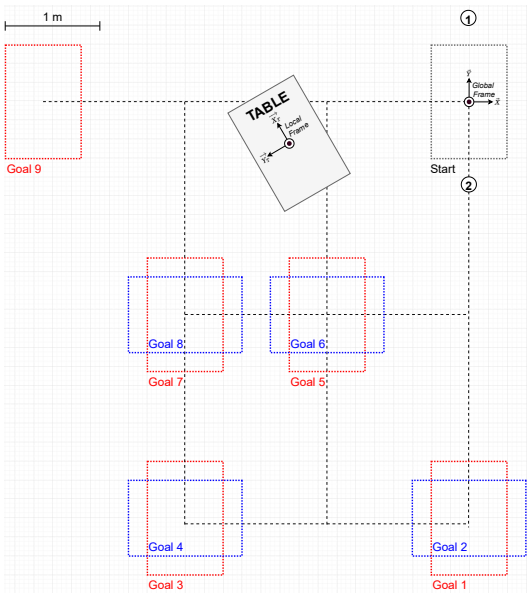

Fig. 3. Starting positions for both subjects (1 and 2 respectively for Subject 1 and Subject 2) and for the table and the 9 different goal positions for the table. The global and local frame are also represented in this figure.

infrared VICON cameras sampled at 200 Hz). The collected data were filtered using a 4th order, zero phase-shift, low-pass Butterworth with a 10 Hz cutoff frequency.

Then, the CoM trajectories of both subjects and of the table, i.e. their CoM horizontal positions (x, y) and their orientations θ with respect to the global frame over each trial, were computed using a previously published method [20]. Let us outline that the table orientation is the orientation of its local frame with respect to the global frame represented in Fig.3. In what follows, a measured table trajectory performed by the j^{th} pair ($j \in [\![1, 20]\!]$) is denoted $X_j^m = \begin{pmatrix} X_{j,1}^m & \dots & X_{j,N}^m \end{pmatrix}$ with N the number of measurements in this trajectory and $\forall i \in [\![1, N]\!]$, $X_{j,i}^m = (x_{j,i}^m, y_{j,i}^m, \theta_{j,i}^m)$. All the measured trajectories were normalized from 0 to 100 % in order to have the same length $N = 500$. For each forward and return paths to and from the same goal position, the average table trajectories $\bar{X}^m$ were computed as follows: $\forall i \in [\![1, N]\!], \bar{X}_i^m = \frac{1}{20} \sum_{j=1}^{20} X_{j,i}^m$.

4) Data analysis: This analysis aims to assess the variability of the table trajectories during various table handling tasks. To this end, we used a metrics first introduced in [18] to compare 2 trajectories X_1 and X_2:

$$\begin{cases} d_{xy}(X_1, X_2) = \frac{1}{N} \sum_{i=1}^{N} \sqrt{(x_{1,i} - x_{2,i})^2 + (y_{1,i} - y_{2,i})^2} \\ d_{\theta}(X_1, X_2) = \frac{1}{N} \sum_{i=1}^{N} |\theta_{1,i} - \theta_{2,i}| \end{cases} \tag{1}$$

d_{xy} and d_θ are respectively named *linear* and *angular distances*. First, the distances between the forward and the return paths were computed for all the pairs. Then, the distances between the average and all the measured forward and return paths were also computed to assess the variability of the measurements with respect to the average trajectories.

5) Results: The first conclusion that can be drawn from the previously described experiments is that the table must be considered as a holonomic system. As a reminder, a holonomic system can take oblique or sideways motion in contrast with non-holonomic systems which always move forward. The table orientation was not always tangent to its trajectory as its is showed in Fig.4. For example, when carried toward Goal 9, the table orientation was orthogonal to its trajectory.

Then, the mean linear and angular distances between the forward and the return paths were respectively 0.17 ± 0.11 m and 0.16 ± 0.14 rad. Both paths would be perfectly symmetrical if those distances were equal to zero. Here it was not the case. However, those means were lower than those observed for non-straight human trajectories [21]. Thus, we can state that the table trajectories were not perfectly symmetrical but they were closer to symmetry than single walking human trajectories.

Furthermore, the linear and angular distances between the individual measurements and their respective average trajectories are represented in Fig.5. On this boxplot, distances for forward and return paths are set apart to check if the results are similar for both directions. A Mann-Whitney U test confirmed this similarity with a p-value greater than 0.05 for both distances. The mean linear and angular distances were respectively 0.13 ± 0.10 m and 0.10 ± 0.12 rad. Moreover, a Kruskal test showed that there is no significant difference between the linear distances for every pair ($p > 0.05$), it was not the case for the angular distances though ($p < 0.01$). This means that the average trajectories were at least representative of all the performed carriages in terms of positions. Thus, in contrast with the subjects trajectories which showed a high variability [17], the table trajectories were more reproducible. As a conclusion, the carriage tasks performed by the different pairs resulted in similar trajectories for the table even if the subjects tended to perform various trajectories themselves. In accordance with this result, in the next section, the focus is on modeling and predicting the table trajectories to allow the robot to act pro-actively during a collaborative table handling task.

B. Modeling

1) Optimal Control (OC) model: The goal of this section is to provide an accurate model of table trajectories between whatever starting and goal positions. Such a model already exists to generate the CoM trajectories of single walking humans. It was adapted from [22] and introduced in [18]. This model is based on the solving of an OC problem using a Differential Dynamic Programming (DDP) algorithm [23] from the open-source Crocoddyl library [24]. This OC problem can generate trajectories of full holonomic systems which follow these dynamics:

$$\begin{cases} \dot{x} = \cos\theta.v_f - \sin\theta.v_o \\ \dot{y} = \sin\theta.v_f + \cos\theta.v_o \\ \dot{\theta} = \omega \end{cases} \quad \begin{cases} \dot{v}_f = u^{v_f} \\ \dot{v}_o = u^{v_o} \\ \dot{\omega} = u^{\omega} \end{cases} \tag{2}$$

With v_f and v_o the forward and orthogonal velocities of the table with respect to orientation of the system and ω the angular velocity.

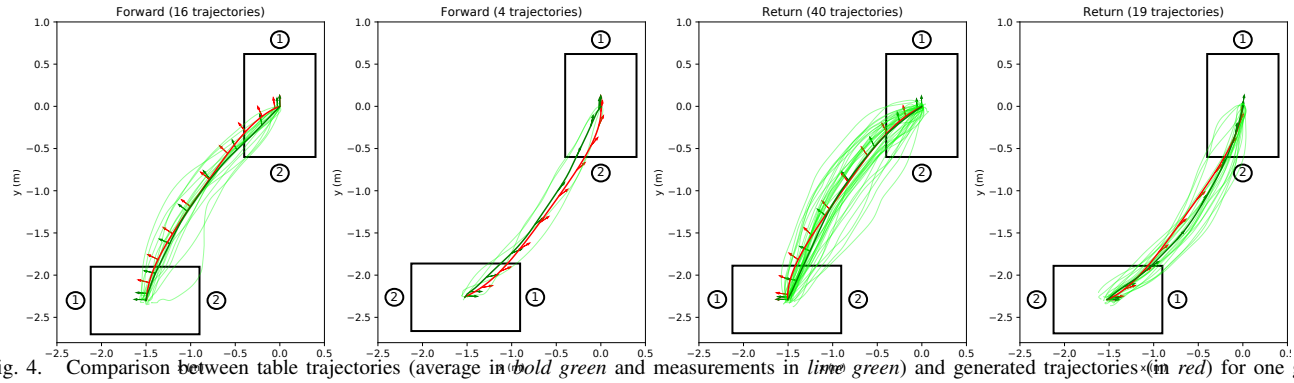

Fig. 4. Comparison between table trajectories (average in *bold green* and measurements in *lime green*) and generated trajectories (in *red*) for one goal position (Goal 8 on Fig.3). The arrows represent the orientation of the table during locomotion and the number 1 and 2 the position of both subjects at the beginning and at the end of the motion.

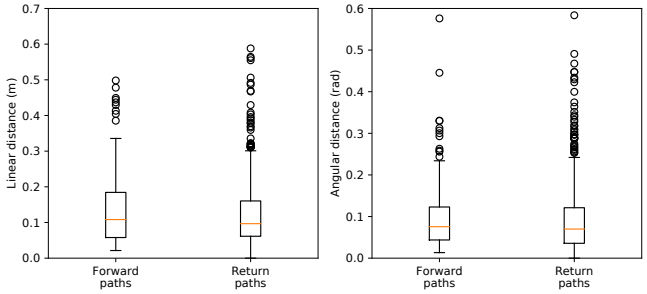

Fig. 5. Linear and angular distances between the individual table trajectories and the average trajectories for every goal.

As human is a holonomic system, this model was suitable to model human CoM trajectories. Then, this OC problem can be described by the following equation:

$$\min_{X(.),U(.),T} \int_0^T \phi_r(X(t),U(t))\,\mathrm{d}t + \phi_t(X(T)) \qquad (3)$$

where $X = \begin{pmatrix} x & y & \theta & v_f & v_o & \omega \end{pmatrix}^T$ and $U = \begin{pmatrix} u^{v_f} & u^{v_o} & u^{\omega} \end{pmatrix}^T$. This problem is solved under two strict equality constraints: the dynamics of the system (Eq.2) and the starting position. The goal position $X_f = (x_f, y_f, \theta_f)$ is a weak constraint expressed in the terminal cost function. The running ϕ_r and terminal ϕ_t cost functions are defined as follows:

$$\begin{cases} \phi_r(X(t),U(t)) = \alpha_0 + \alpha_1 u^{v_f 2}(t) + \alpha_2 u^{v_o 2}(t) + \alpha_3 u^{\omega 2}(t) \\ \qquad\qquad +\alpha_4 \psi(X(t),X_f)^2 \\ \phi_t(X(T),U(T)) = \beta_0(\Delta_x^2 + \Delta_y^2) + \beta_1 \Delta_\theta^2 + \beta_2(v_f(T)^2 \\ \qquad\qquad +v_o(T)^2) + \beta_3 \omega(T)^2 \end{cases} \qquad (4)$$

In this equation, $\Delta_\nu = \nu_f - \nu(T)$ with $\nu \in \{x, y, \theta\}$ and ψ is a function to simulate the asymmetry between back and forth trajectories. In [18], an Inverse Optimal Control (IOC) scheme was proposed to optimized the weights of the running ϕ_r and terminal ϕ_t cost functions, respectively $\alpha = (\alpha_0, \alpha_1, \alpha_2, \alpha_3, \alpha_4)$ and $\beta = (\beta_0, \beta_1, \beta_2, \beta_3)$. As it gave accurate results for single walking humans and as a table carried by two humans is also a holonomic system (Sec.II-A.5), the choice was made to apply the same method to model the table trajectories. The optimal trajectories generated with this OC model are denoted $X^g = \begin{pmatrix} X_1^g & \dots & X_N^g \end{pmatrix}$. We assumed that the generated trajectories have the same length as the measurements. It was not necessarily the case, but, when it was not, the generated trajectory were interpolated to count N points.

2) IOC results: The IOC scheme, detailed in [18], was used to optimized the cost functions weights in order to minimize the linear and angular distances between the average table trajectories and the trajectories generated with the OC problem described in Eq.3. The weights which allow the best fitting of average and generated trajectories are the followings:

$$\begin{cases} \alpha \approx (3.01 \times 10^{-3}, 6.03, 5.99, 8.63 \times 10^{-2}, 1.00 \times 10^{-7}) \\ \beta \approx (9.98, 7.99, 14.99, 0.42) \end{cases} \qquad (5)$$

One can denote that the weight α_4, which weights the asymmetry of the back and forth trajectory, is close to 0. This confirms the conclusion made in Sec.II-A.5. Thus, the table trajectories are more symmetrical than the humans' ones for which $\alpha_4 = 10$ [18]. Then, using these new sets of weights in the OC cost functions, the table trajectories between the experimental starting position and all the goal positions were generated for the forward and the return paths.

3) Comparison with measurements: All the measured, average and generated trajectories to go and return from one given goal are represented in Fig.4. On this figure, the generated trajectories are quite accurate. To confirm this guess, $d_{xy}(X^m, X^g)$ and $d_\theta(X^m, X^g)$ were computed for every forward and return paths. The linear and angular distances respectively amounted to 0.12 ± 0.12 m and 0.36 ± 0.61 rad. All the results are represented in Fig.6. As for the measured data, no significant difference existed between the results for the forward and the return paths (Mann-Whitney U test, $p > 0.05$). Thus, the distances were of the same magnitude as the ones computed between the average and the measured trajectories. Moreover, a Kruskal test demonstrated that the linear distances between the average and measured trajectories were non-distinguishable from the linear distances between the average and the generated trajectories ($p > 0.05$). However, that was not the case for angular distances. Thus, on one hand, we can conclude that the presented OC model provides accurate trajectories in terms of x and y coordinates. On the other hand, the generated orientations might not be always accurate. Thus, we built an

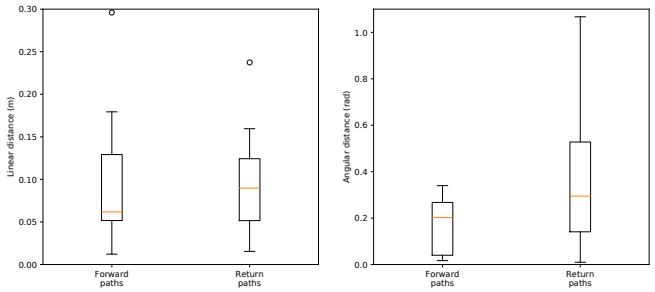

Fig. 6. Linear and angular distances between the individual table trajectories and the average trajectories for every goal.

OC model which accurately simulates average paths of the table given whatever starting and goal positions. However, during a human-robot table handling task, the robot may not know the goal position or may have to adapt to an atypical behaviour. Thus, the next section focuses on the prediction of where the table is going according to the table current and recent past positions.

C. Prediction process

1) Prediction model: In [16], a prediction process was designed to predict the future CoM trajectory of a walking subject from its recent past trajectory of size N_0. We assumed that the trajectory is recorded in real-time at a rate of $\frac{1}{T_{OC}}$. This process is based on the solving of a similar OC problem to the one used to generate the trajectories of single walking humans in [18]. In the previous section, we demonstrated that the same model, with different weights (Eq.5), succeeded in generating the trajectories of a table handled by two subjects. Thus, the same OC problem can be used to predict the table trajectories with identical running and terminal cost functions.

At each time $t = kT_{OC}$ ($k = n + N_0$), this OC problem fits the recent past trajectory $\begin{pmatrix} X^m_{n+1} & \dots & X^m_k \end{pmatrix}^T$ and generates a trajectory of size N_{OC}, denoted $\tilde{X}^*_{n+1} = \begin{pmatrix} X^*_{n+1} & \dots & X^*_k & \dots & X^*_{n+N_{OC}} \end{pmatrix}^T$. In this solution, the *predicted trajectory* is $\begin{pmatrix} X^*_k & \dots & X^*_{n+N_{OC}} \end{pmatrix}^T$. N_{OC} should be greater than N_0 so that the predicted trajectory exists. An example of the trajectory generated with this OC prediction problem is shown in Fig.7. More details about this prediction process are available in [16].

2) Assessment: Then, the accuracy of the predicted trajectory of the table was assessed with the same metrics used in [19]. At each time, for each measured table trajectory, the predicted trajectory was computed along with the linear and angular distances between this prediction and the real performed trajectory. Moreover, the predicted distance d_{pred}, which is defined as the Euclidean distance between X^*_k and $X^*_{n+N_{OC}}$, namely between the first and the last point of the predicted trajectory, was also computed. This distance is represented in Fig.7. The averages of these distances for all the measurements are presented in Tab.I for multiple values of N_0 and N_{OC}. This table shows better results than the one obtained for single walking humans [19]. Even if the predicted distances are lower, the linear and, especially, the angular distances demonstrate better accuracy. Moreover, it is interesting to denote that those linear and angular distances are low enough to expect an accurate and reactive prediction of where the human wants to carry the table during the targeted collaborative table handling task.

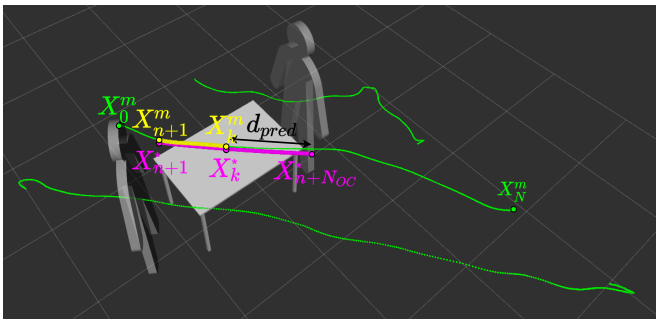

Fig. 7. Predicted trajectory at time $t = kT_{OC}$ with $N_0 = 50$ and $N_{OC} = 100$ for one given trial. The measured trajectories of both subjects and of the table are in *green*, the recent past trajectory of the table is in *yellow* and the solution provided by the prediction process is in *purple*.

N_0	N_{OC}	d_{xy} (m)	d_θ (rad)	d_{pred} (m)
25	100	0.08 ± 0.07	0.08 ± 0.09	0.74 ± 0.32
50	100	0.04 ± 0.02	0.04 ± 0.02	0.45 ± 0.11
50	200	0.07 ± 0.07	0.07 ± 0.06	0.76 ± 0.37

TABLE I

AVERAGE DISTANCES FOR VARIOUS N_0 AND N_{OC}.

III. WALKING WITH THE TABLE

A. Coupling of the prediction process and the robot WPG

The same WPG as the one introduced in [16] is used in this paper. This WPG generates the CoM and the feet trajectories of a humanoid robot along a given trajectory by solving a Non-linear Model Predictive Control (NMPC) problem. When the trajectory given as an input to the WPG is the real-time solution of the prediction process, the WPG is said to be coupled with the prediction process. In this work, the input given to the WPG is the table predicted trajectory translated so that the robot is placed on the free side of the table. Moreover, this trajectory is interpolated in order to be traveled at a the measured table velocity. More details about this interpolation are given in [16]. Two examples of CoM and footsteps generated with this WPG are shown in Fig.8.

The source code resulting in these simulations is open-source and available on: `https://github.com/imaroger/table_trajectories_during_collaborative_carriage`.

B. Whole-body controller of the robot

Once the CoM and the footsteps trajectories are computed, they have to be executed on the robot through a whole-body controller. In this article, we used the torque controller introduced in [25], [26]. It is a weighted quadratic program based on the Task Space Inverse Dynamic (TSID) library [27]. This controller computed stable torque commands for all the joints of the robot from the reference trajectories generated by the WPG and the current state of the robot. These commands were sent to the simulated robot at 1 kHz. To achieve

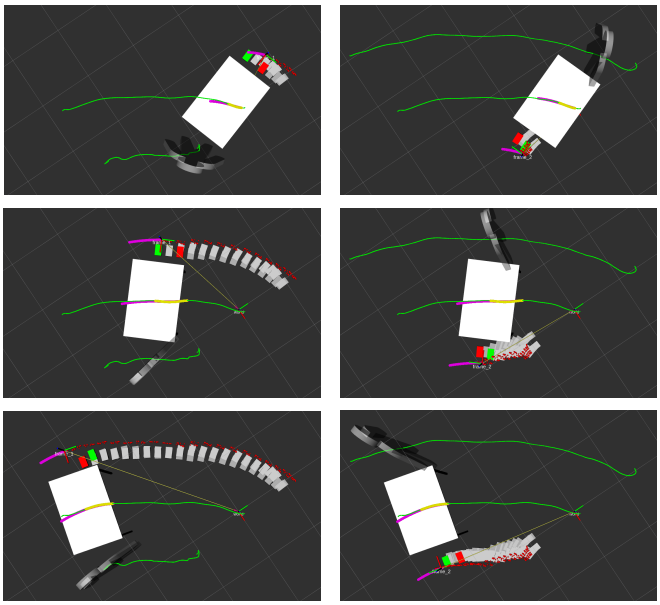

Fig. 8. The robot CoM (in *red*) and footsteps (past steps in *grey*, current support foot in *red* and future support foot in *green*) are generated from the predicted table trajectory (in *purple*) with $N_0 = 50$ and $N_{OC} = 100$. On the left, the robot substitutes Subject 1 while, on the right, it substitutes Subject 2.

this rate, the trajectories computed by the WPG had to be interpolated using polynomial functions.

This controller was used not only to make the robot walk but also to make the robot lift the table. Indeed, in addition to the tasks ensuring the tracking of the reference trajectories, the contacts on the floor and the robot's balance, a posture task was added to make the robot fetch and grab the table. At first, this task made the robot lower it CoM and align its gripper with the table legs in front of it. Then, this task was updated to make the robot close its gripper and return to its initial CoM height. Thus, this posture task forced the robot's hands to stay closed while walking as it is shown in Fig.1.

C. Simulation of the collaborative table handling task

The last step of this paper is to test the whole framework described in the previous sections in simulations. They are aimed to be as realistic as possible. For example, in the simulations, the 3D model of the table had the same characteristics (length, width, height and weight) as the real one carried by the subjects in the experiments presented in Sec.II-A.

The simulations realized in this article were run on Gazebo on a standard laptop (Intel(R) Core(TM) i5-8400H CPU @ 2.50GHz). The challenges of these simulations were twofold. First, the impact of the human on the table needed to be simulated to create a haptic interaction with the robot through the table. Then, the whole body controller needed to keep the robot's balance despite the perturbations induced by the table.

1) Simulation of the human partner: To achieve the simulation of a human-robot collaborative carriage, the robot behaviour was not the only one which needed to be simulated

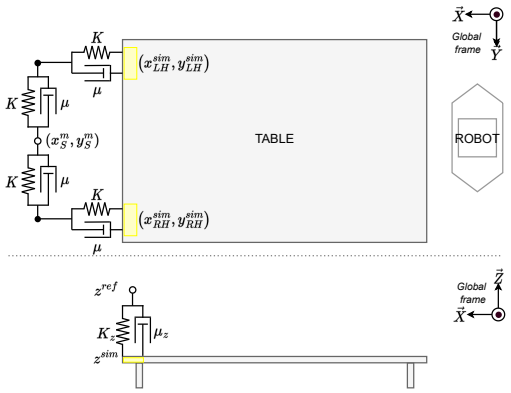

Fig. 9. Simulation of the human partner with a spring-mass-damper system to hold the table on Gazebo.

in Gazebo. Indeed, the impact of the human on the carried load also needed to be simulated. As no force sensor was used during the experiments described in Sec.II-A, only the recorded CoM trajectories of the subjects could be used to mimic the haptic feedback produced by the subject during a table handling task. In [28], the authors studied a collaborative carriage where two subjects carried a stretcher-like object. The motions of the subjects were recorded also as the force data on each handle. Then, a comparison between these data and the solutions of paired Spring Loaded Inverted Pendulums (SLIPs) demonstrated that this SLIPs model can reproduce human walking behaviour during a collaborative carriage. Based on this conclusion, in the simulation presented in this paper, the human partner was simulated using spring-mass-damper systems as represented in Fig.9. Using the ROS [29] service `/gazebo/apply_body_wrench`, forces were applied on the yellow spots in Fig.1 and Fig.9 to simulate the human right and left hands on the table. They are denoted $\overrightarrow{F_\nu} = F_{\nu,x}\overrightarrow{X} + F_{\nu,y}\overrightarrow{Y} + F_{\nu,z}\overrightarrow{Z}$ with $\nu \in \{RH, LH\}$ and they are defined as follows:

$$\begin{cases} F_{\nu,x} = -K(x_\nu^{sim} - x_S^m) - \mu v_{\nu,x}^{sim} \\ F_{\nu,y} = -K(y_\nu^{sim} - y_S^m) - \mu v_{\nu,y}^{sim} \\ F_{\nu,z} = -K_z(z_\nu^{sim} - z^{ref}) - \mu_z v^{ref} \end{cases} \quad (6)$$

$(x_\nu^{sim}, y_\nu^{sim}, z_\nu^{sim})$ are the 3D positions in the global frame of the yellow spots measured by Gazebo and streamed on the topic `/gazebo/link_states`, (x_S^m, y_S^m) is the measured horizontal position in the global frame of the subject and $z^{ref} = 0.9$ m is the reference height where we want the table to be. The stiffness and damping coefficients were heuristically found: $K = 1$, $\mu = 4$, $K_z = 300$ and $\mu_z = 50$.

2) Results: Simulations for various measured table trajectories were successfully achieved. A video showing one simulation is available on: `https://peertube.laas.fr/videos/watch/a2382b7e-4a7f-454b-8dcc-6c93b27a8a50`. Those different simulations succeeded whoever (Subject 1 or Subject 2) the robot substituted. This result is interesting as it demonstrates that the robot can carry the table with its simulated partner walking forward and walking backward. Moreover, the robot's balance was not disturbed by the

table. Indeed, the forces measured by the 6-axis force sensors in both ankles showed similar profiles whether the robot walks with or without the table. This means that the controller properly compensated for the perturbations induced by the table.

IV. Discussion

In this article, a prediction model of table CoM trajectories during various collaborative handling tasks is designed based on the one introduced in [16]. Once coupled to a TALOS robot WPG it allows the robot CoM and footsteps to follow the predicted trajectory of the table. Doing so, in simulation, the robot can anticipate the table motions. Thus, embedding the predicted table behaviour into the robot planner allows the robot to assist actively its human partner instead of passively follow its motions.

Table trajectories versus human trajectories. Interesting conclusions can be drawn from the table trajectories and from the assessment of the prediction model. The table trajectories presented a lesser variability compared to the subjects trajectories. This resulted in the building of an OC model which accurately fit the average measurements. Moreover, the prediction of table trajectories were closer to the measurements than the prediction of single walking human trajectories [19]. Two phenomena could explain those results. First, as the table was heavy (20.7 kg) and cumbersome ($1.22 \times 0.8 \times 0.77$ m), the subjects may want to reduce the amplitude of the table motions. By doing so, they may optimize the table trajectory rather than their own. This may explain why the IOC succeeded here while the same scheme failed to find optimal cost function weights to model the subjects' trajectories [17]. Then, The table trajectories were smoother than human trajectories as they were not subject to the CoM oscillations induced by footsteps which can be observed when studying human trajectories. Thus, as the OC problems modeling and predicting trajectories did not take into account these oscillations, they may work better on table trajectories rather than on human trajectories.

Realism of the forces applied on the table in the simulation. First of all, the simulation of the human with spring-mass-damper systems depended on the values of the stiffness and damping coefficients. As already stated, those coefficients were heuristically found. They were chosen because they resulted in consistent behaviour of the table when two simulated humans carried the table in terms of the performed trajectory and the travel speed. In this study, we checked that the trajectory performed by the table with spring-mass-systems linked to the measured positions of the subjects on both sides of the table was similar to the respective measured one. However, as we did not have measured forces data during the recorded table handling tasks, it is unclear if the forces applied on the table to simulate the human partner were of the same magnitude as the ones a real human would apply. Ongoing works are investigating this issue.

Finally, let us denote that in Fig.1, two forces of 15 N each are represented on the yellow spots on the side of the table held by the robot. Those forces, applied on the table using the ROS service `/gazebo/apply_body_wrench`, were not realistic. Indeed, if it was not a simulation, no one else than the robot could apply forces on this side of the table. However, in the simulation, if those forces were not applied, the robot was not able to lift the table. It was probably due to the torque control, which was too soft. Indeed, former experiments, in position control, already showed that the robot was strong enough to lift and hold this 20.7 kg table with a human partner. However, the fact that the robot was position-controlled made the robot stiffer. In future works, the stiffness in the robot arms could be increased by adding an impedance task at the hand level, this may ensure a stiffer behaviour along the vertical axis. This task will be implemented later, for now, we assume that those 15 N forces are a good approximation of this task. Moreover, it is important to denote that the robot still carried between 60 and 80 N. This force was measured using the 6-axis force sensors in the robot hands. This demonstrated the ability of the robot to carry a quite heavy table with a human partner.

Walking patterns achieved on the simulated robot. In this work, the footsteps performed in simulation were more challenging than the ones tested in [16], [25], [26]. Indeed, some tested trajectories included large sideways or backward steps and significant rotations of the feet. Those kinds of motions have not been tested with the used torque controller before. To achieve those motions, the time of the double support phase had to be increased from 0.2 s to 0.3 s. Thus, in all the simulations presented in this paper, the sampling period time of the NMPC was 0.3 s, the size of the preview horizon was 16 and the duration of one step was 2.4 s. With those parameters, footsteps up to 0.4 m were generated. Moreover, in [16], the NMPC became unfeasible if the trajectory to track had a non-zero curvature and had to be quickly traveled. This problem was avoided, in this work, by changing the weights in the cost function of the NMPC. In particular, the weight ensuring that the Zero Moment Point (ZMP) is under the ankle was increased. This resulted in no more unfeasibility problems. However, when the velocity to travel the trajectory was higher than 0.2 m.s^{-1}, the predicted trajectory was not well tracked. Thus, we simulated the robot following the predicted table trajectories for a table moving at a maximum velocity of 0.2 m.s^{-1}.

Toward a real-time experiment on the real robot. A few challenges remain to face in order to perform a real pro-active human-robot collaborative carriage. For example, the duration of one iteration of the NMPC was around 0.03 s. Nevertheless, to be embedded in real-time on the real robot, the duration of one iteration should be around 0.005 s. Currently, the NMPC is implemented in Python. An implementation in Cython was tested to speed up the NMPC. However, the duration only decreased by 40%. In current work, the WPG is being coded in C++ to decrease the computation time. Once this work done, an online version of the WPG will be plugged into the whole-body controller and tested on the real robot.

Moreover, the simulations achieved in this paper demonstrated that, using a prediction of the table trajectory, a humanoid robot can follow this trajectory. By doing so, it can be active during the carriage anticipating where its partner wants to set the table. It would be interesting, in future works, to assess the impact of using predicted trajectories on the robot's reactivity compared to using minimal distance trajectories or other heuristics. Moreover, two flaws might prevent real pro-active interaction. First, in this article, the predicted trajectory was computed from the recent past trajectory of a table carried by two subjects. If one of the subjects is replaced by the robot, the table may not take the same trajectory. In this situation, we expect that the initial motion given by the human to the table will be enough for the prediction process to start predicting a trajectory to give to the robot. Once the robot is walking, it should give to the table a motion that looks like the motion a human would have given. Nevertheless, as we cannot perform a real experiment yet, we cannot check if the prediction model will behave as expected. Furthermore, as previously stated, the robot cannot walk faster than 0.2 m.s^{-1}. During the experiments, the pairs made the table move at average velocities between 0.35 and 0.8 m.s^{-1}. Thus, with the current WPG, a humanoid robot cannot actively assist a human partner as it cannot walk as fast as its partner. Thus to target a pro-active carriage task, the embedding of the table prediction into a robot planner will be more relevant on a faster robot like a wheeled robot, for example.

V. Conclusion

In this paper, a framework allowing a pro-active human-robot collaborative carriage is presented. This framework includes a prediction model of table trajectories during various carriage tasks. This model was designed using data measured during human-human table handling tasks as part of this study. It is based on a similar OC model to the one designed to predict single walking human trajectories [16], except that the cost function weights were optimized to fit the measured table trajectories. The assessment of this new model demonstrated that it accurately predicted the future table trajectory from its recent past trajectory. Thus, this prediction was coupled with the TALOS robot WPG in order to embed the table behaviour into the robot CoM and footsteps planner. Then, a torque whole-body controller was used to send torque command to the robot join in order to follow the CoM and feet trajectories generated by the WPG. Once the robot controlled on Gazebo, the force applied on the table by the human partner were simulated using spring-mass-damper systems. Finally, this whole framework was successfully tested in simulation on Gazebo. Future works will target experiments on the real robot.

References

[1] N. Jarrassé, V. Sanguineti, and E. Burdet, "Slaves no longer: review on role assignment for human–robot joint motor action," in *Adaptive Behavior, SAGE Publications*, 2013.

[2] A. Ajoudani, A. M. Zanchettin, S. Ivaldi, A. Albu-Schäffer, K. Kosuge, and O. Khatib, "Progress and prospects of the human–robot collaboration," *Autonomous Robots*, 2018.

[3] N. Stergiou and L. M. Decker, "Human movement variability, nonlinear dynamics, and pathology: Is there a connection?" *Human Movement Science*, 2011.

[4] A. Bussy, A. Kheddar, A. Crosnier, and F. Keith, "Human-humanoid haptic joint object transportation case study," in *IEEE IROS*, 2012.

[5] J. Lanini, H. Razavi, J. Urain, and A. Ijspeert, "Human intention detection as a multiclass classification problem: Application in physical human–robot interaction while walking," in *IEEE RA-L*, 2018.

[6] K. Otani, K. Bouyarmane, and S. Ivaldi, "Generating assistive humanoid motions for co-manipulation tasks with a multi-robot quadratic program controller," in *IEEE ICRA*, 2018.

[7] M. Sharifi, S. Behzadipour, and G. Vossoughi, "Nonlinear model reference adaptive impedance control for human–robot interactions," in *Control Engineering Practice*, 2014.

[8] D. J. Agravante, A. Cherubini, A. Bussy, P. Gergondet, and A. Kheddar, "Collaborative human-humanoid carrying using vision and haptic sensing," in *IEEE ICRA*, 2014.

[9] S. Lo, C. Cheng, and H. HP., "Virtual impedance control for safe human-robot interaction," in *Journal of Int. & Rob. Systems*, 2016.

[10] A. Dutta and O. Obinata, "Impedance control of a robotic gripper for cooperation with humans," in *Control Engineering Practice*, 2002.

[11] E. Gribovskaya, A. Kheddar, and A. Billard, "Motion learning and adaptive impedance for robot control during physical interaction with humans," in *IEEE ICRA*, 2011.

[12] A. Fishman, C. Paxton, W. Yang, D. Fox, B. Boots, and N. Ratliff, "Collaborative interaction models for optimized human-robot teamwork," in *IEEE IROS*, 2020.

[13] A. Bussy, P. Gergondet, A. Kheddar, F. Keith, and A. Crosnier, "Proactive behavior of a humanoid robot in a haptic transportation task with a human partner," in *IEEE ROMAN*, 2012.

[14] P. Mohammadi, E. M. Hoffman, L. Muratore, N. G. Tsagarakis, and J. J. Steil, "Reactive walking based on upper-body manipulability: An application to intention detection and reaction," in *IEEE ICRA*, 2019.

[15] T. Kobayashi, E. Dean-Leon, J. R. Guadarrama-Olvera, F. Bergner, and G. Cheng, "Multi-contacts force-reactive walking control during physical human-humanoid interaction," in *Humanoids*, 2019.

[16] I. Maroger, N. Ramuzat, O. Stasse, and B. Watier, "Human trajectory prediction model and its coupling with a walking pattern generator of a humanoid robot," *IEEE RA-L*, 2021.

[17] I. Maroger, M. Silva, H. Pillet, N. Turpin, O. Stasse, and B. Watier, "Walking paths during collaborative carriages do not follow the simple rules observed in the locomotion of single walking subjects," in *Scientific Reports*, 2022.

[18] I. Maroger, O. Stasse, and B. Watier, "Inverse optimal control to model human trajectories during locomotion," *CMBBE*, 2021.

[19] I. Maroger, , O. Stasse, and B. Watier, "Description and assessment of a human trajectory prediction model during gait," *SB*, 2021.

[20] M. Saini, D. C. Kerrigan, M. A. Thirunarayan, and M. Duff-Raffaele, "The vertical displacement of the center of mass during walking: A comparison of four measurement methods," *Journal of Biomechanical Engineering*, 1998.

[21] M. Sreenivasa, K. Mombaur, and J.-P. Laumond, "Walking paths to and from a goal differ: On the role of bearing angle in the formation of human locomotion paths," *PLOS ONE*, 2015.

[22] K. Mombaur, A. Truong, and J.-P. Laumond, "From human to humanoid locomotion—an inverse optimal control approach," *Autonomous Robots*, 2010.

[23] Y. Tassa, N. Mansard, and E. Todorov, "Control-limited differential dynamic programming," in *IEEE ICRA*, 2014.

[24] C. Mastalli, R. Budhiraja, W. Merkt, G. Saurel, B. Hammoud, M. Naveau, *et al.*, "Crocoddyl: An efficient and versatile framework for multi-contact optimal control," in *IEEE ICRA*, 2020.

[25] N. Ramuzat, G. Buondonno, S. Boria, and O. Stasse, "Comparison of position and torque whole-body control schemes on the humanoid robot talos," in *IEEE ICAR*, 2021.

[26] N. Ramuzat, O. Stasse, and S. Boria, "Benchmarking whole-body controllers on the talos humanoid robot," *Frontiers*, 2022.

[27] A. Del Prete, N. Mansard, O. E. Ramos, O. Stasse, and F. Nori, "Implementing torque control with high-ratio gear boxes and without joint-torque sensors," in *Int. Journal of Humanoid Robotics*, 2016.

[28] J. Lanini, A. Duburcq, H. Razavi, C. G. Le Goff, and A. J. Ijspeert, "Interactive locomotion: Investigation and modeling of physically-paired humans while walking," *PLOS ONE*, 2017.

[29] Stanford Artificial Intelligence Laboratory et al., "Robotic operating system." [Online]. Available: https://www.ros.org